

mediate vicinity of 2.41 Mev, the nearest  $\gamma$ -ray energy being at 2.50 Mev. Because of its extreme sharpness, the maximum may have escaped detection in the photo cross section measurements.

Longmire has chosen the  $D_{5/2}$  state as the final state for the following reasons: (1) The virtual levels belonging to states of lower orbital angular momentum are too broad to explain the sharpness of the observed maximum. (2) The  $D$  level is presumed to be the lowest energy level which is sufficiently narrow to meet the requirements of the empirical data. The  $D_{5/2}$  level is assumed to be of lower energy than the  $D_{3/2}$  level; this is to be expected on the basis of relativistic spin-orbit coupling. (3) The matrix elements corresponding to a change of the angular momentum of the incident proton by more than one unit are small. Longmire chooses the well describing the  $\text{Be}^8$ -neutron interaction in the  $D_{5/2}$  state in such a way that the virtual  $D_{5/2}$  level is ex-

tremely narrow. Unfortunately, the theory of the photo-disintegration of  $\text{Be}^9$  seems to require that the  $D_{5/2}$  level be a broad level centered at an energy considerably higher than 2.41 Mev. A reasonable solution to this problem is to assume the sharp maximum in the proton scattering data to be due to a  $P \rightarrow F$  transition. On the assumption that the  $\text{Be}^8$ -neutron interaction is partly of a Majorana type, it is not at all unreasonable to have the  $F$  level at a lower energy than the  $D$  level. Furthermore, even though the matrix elements for the  $P \rightarrow F$  transition may be small for most energies, a sharp resonance at the narrow  $F$  level could result in the sharp maximum observed.

#### ACKNOWLEDGMENT

The authors wish to thank Mr. G. S. Colladay for the computation of most of the numerical results used in the paper.

## The $(\alpha, n)$ Cross Section of Boron\*

R. L. WALKER\*\*

*University of California, Los Alamos Scientific Laboratory, Los Alamos, New Mexico*

(Received March 21, 1949)

The differential cross section for the  $\text{B}^{10,11}(\alpha, n)\text{N}^{13,14}$  reactions was measured as a function of the alpha-particle energy up to an energy of 5.3 Mev. To determine this cross section, the number of neutrons emitted by boron under alpha-particle bombardment was measured by comparison with a calibrated Ra- $\alpha$ -Be source in a graphite column.

Resonances were observed at alpha-particle energies of 1.8, 2.5, 4.2, 4.9 Mev. Poor resolution may explain why other resonances found by Maurer and by Fünfer were not observed.

### I. INTRODUCTION

NEUTRONS are produced when alpha-particles strike boron, by the two reactions:

$$\begin{aligned} \text{B}^{11} + \text{He}^4 &= \text{N}^{14} + n & Q &\approx + .28 \text{ Mev.} \\ \text{B}^{10} + \text{He}^4 &= \text{N}^{13} + n & Q &\approx + 1.2 \text{ Mev.} \end{aligned}$$

Reasons are given by Bonner and Mott-Smith<sup>1</sup> and by Maurer<sup>2</sup> for believing that only a small fraction of the neutrons from boron (of the order of one-tenth) arise from  $\text{B}^{10}$ . Thus the principal neutron yield from boron under alpha-particle bombardment is probably due to the first reaction above.

Maurer<sup>2</sup> and Fünfer<sup>3</sup> have studied the  $\text{B}^{10,11}(\alpha, n)\text{N}^{13,14}$  reactions at different alpha-particle energies for the purposes of locating resonances, determining upper

limits for their widths and determining the level spacing of the intermediate nucleus for the first reaction,  $\text{N}^{13}$ .

In the present work an absolute measurement of the cross section for the  $\text{B}^{10,11}(\alpha, n)\text{N}^{13,14}$  reactions was made by determining the number of neutrons emitted from a thin boron target upon which are incident a known number of alpha-particles of variable energy.

### II. EXPERIMENTAL ARRANGEMENT

The conventional arrangement shown in Fig. 1 was used as a means of controlling the energy of the alpha-particles striking the boron target. Alpha-particles from polonium coated on the small central sphere, 5 mm in diameter, lose a part of their energy in nitrogen gas before striking the thin boron target coated on the inside of two hemispherical iron spinings, 7.5 cm in diameter. By changing the pressure of nitrogen in the chamber one can control the energy of the alpha-particles when they reach the boron.

The assembly shown in Fig. 1 was placed in a graphite column containing a sensitive  $\text{BF}_3$  proportional counter, in order that the number of neutrons emitted by the

\* This paper is based on work performed at Los Alamos Scientific Laboratory of the University of California under contract No. W-7405-eng-36 for the Manhattan Project.

\*\* Now at Cornell University, Ithaca, New York.

<sup>1</sup> T. W. Bonner and L. M. Mott-Smith, Phys. Rev. **46**, 258 (1934).

<sup>2</sup> W. Maurer, Zeits. f. Physik **107**, 721 (1937).

<sup>3</sup> E. Fünfer, Ann. d. Physik **35**, 147 (1939).

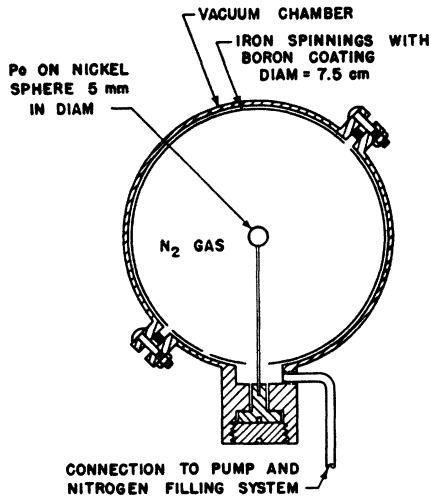


FIG. 1. Experimental arrangement of the alpha-particle source and the boron target.

boron might be measured as a function of the nitrogen pressure in the chamber. The neutron measurement will be described later.

Data on the polonium sources and the boron targets used are collected in Tables I and II. The polonium sources were made by Mr. Leonard Treiman of Dr. Martin's group at Los Alamos. The sources were placed in the nitrogen atmosphere of the chamber immediately after the polonium was deposited in order to avoid oxidation, and all the data were taken within one or two days thereafter. The sources were then returned to Mr. Treiman, who measured their strengths by a calorimeter method.

The boron layers were coated on the iron hemispheres by Mr. Glenn Barbaras and Dr. W. P. Jesse at the Metallurgical Laboratory of the University of Chicago. In the process both sides of the hemispheres were coated. Since only the total amount deposited could be found by weighing, the weight of boron on the inside surface,

TABLE I. Data on the polonium sources.

Po source	Strength when made (curies)	Thickness (curies/cm <sup>2</sup> )	Thickness (cm air equivalent)*
1	1.55	1.96	0.11
3	0.48	0.61	0.033

\* Using 4.2 for the atomic stopping power of polonium relative to air for alpha-particles of energy near 5 Mev.

TABLE II. Data on the boron targets.

Boron layer	Total weight of boron on inside surface (mg)	Thickness (mg/cm <sup>2</sup> )	Equivalent air thickness* (cm air)
"Thicker boron"	56	0.31	0.33
"Thinner boron"	31	0.18	0.18

\* Using 0.94 for the atomic stopping power of boron relative to air.

as shown in Table II, involves an estimate that 55 percent of the total weight was on the inside.

III. ALPHA-PARTICLE ENERGY. RESOLUTION

The alpha-particle energy corresponding to a given pressure of nitrogen in the chamber was found from the range-energy relation given by Holloway and Livingston<sup>4</sup>, assuming the atomic stopping power of nitrogen relative to air to be 0.99.

The resolution was limited by the spread in the energies of the alpha-particles resulting from the finite thickness of the boron target, the thickness of the polonium source, the straggling of the energy loss, and the differences in the geometrical path lengths through the nitrogen gas. In Table III are listed estimates of the loss of resolution from these causes. The effect of the source thickness was calculated assuming the polonium layer to be pure and of uniform thickness. The energy spread in Table III is such that, under the assumed conditions, about 85 percent of the alpha-particles emitted have energies differing from the maximum energy by less than the amount listed.

IV. NEUTRON MEASUREMENT

The chamber containing the Po source and boron target was placed on the axis of a large graphite column (approx. 5x5x9 feet) with a sensitive BF<sub>3</sub> proportional counter about 58 cm away from the chamber,

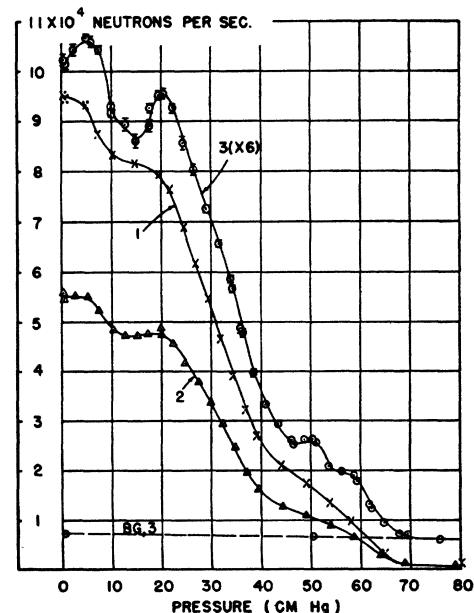


FIG. 2. Number of neutrons emitted in the  $B^{10,11}(\alpha,n)N^{13,14}$  reactions as a function of the pressure of nitrogen in the chamber. Curve 1: Po source No. 1 and "thicker" boron target. Curve 2: Po source No. 1 and "thinner" boron target. Curve 3: (ordinates multiplied by 6): Po source No. 3 and "thinner" boron target. The background for curve 3 is shown by the curve marked BG,3.

<sup>4</sup>M. G. Holloway and M. S. Livingston, Phys. Rev. 54, 18 (1938).

TABLE III. Estimates of the loss of resolution from various causes.

Alpha-particle energy (Mev)	Energy spread due to source thickness (Mev)		Straggling of energy loss (Mev)	Energy loss in boron target (Mev)		Energy spread due to differences in path lengths (Mev)
	Po source No. 1	Po source No. 3		"Thicker boron"	"Thinner boron"	
1	0.5	0.13	0.11	0.72	0.41	0.32
2	0.5	0.13		0.60	0.34	0.24
3	0.5	0.13		0.46	0.26	0.14
4	0.5	0.13		0.40	0.22	0.07
5	0.5	0.13	0.03	0.32	0.18	0.01

also on the axis of the column. With this separation between the neutron source and slow neutron detector, the counting rate is relatively insensitive to the primary energy of the neutrons emitted by the source, being approximately proportional to the number of neutrons emitted per second (see Appendix). Assuming this proportionality to be exact, the neutron measurement is easily made absolute by observing the counting rate of the  $BF_3$  counter when the polonium alpha-particle source is replaced by a Ra- $\alpha$ -Be neutron source of known strength. In this way, the number of neutrons emitted from the boron under alpha-particle bombardment was measured as a function of the pressure of nitrogen in the chamber. Data are shown in Fig. 2 for three combinations of Po source and boron target, corresponding to different energy resolutions. The probable error in the absolute calibration of the Ra- $\alpha$ -Be source used as a standard was about 5 percent.<sup>5</sup>

Background of neutrons from impurities in the Po source, from the nitrogen gas, or from the iron hemispheres upon which the boron was deposited, was meas-

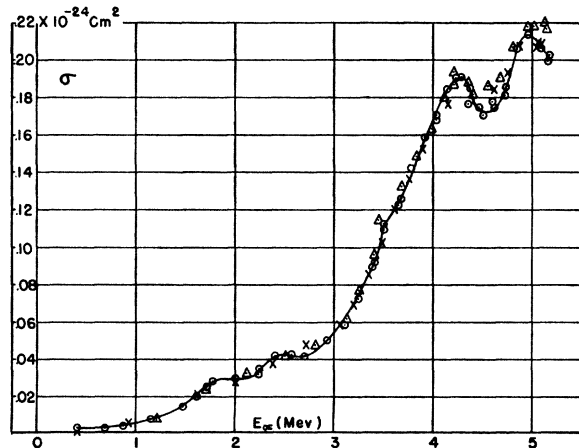


FIG. 3. Cross section for the  $B^{10,11}(\alpha,n)N^{13,14}$  reactions as a function of the alpha-particle energy. The curve has been drawn through data obtained with the best resolution, i.e., with Po source No. 3 and the "thinner" boron target (circles). Also shown are data obtained with Po source No. 1 and the "thinner" boron target (triangles), and with Po source No. 1 and the "thicker" boron target (crosses).

<sup>5</sup> O. R. Frisch and R. L. Walker, Los Alamos Declassified Report LADC-155 (1945).

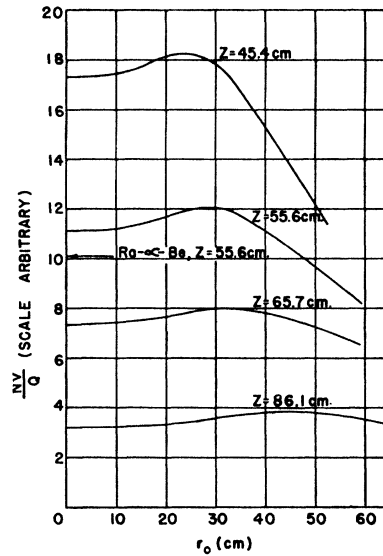


FIG. 4. Flux of thermal neutrons as a function of the parameter  $r_0$  of the source function.  $Z$  is the distance from the source along the axis of the graphite column. The arrow marked "Ra- $\alpha$ -Be" indicates the value of  $nV/Q$  calculated from a measured distribution  $q$  for one Ra- $\alpha$ -Be source, at  $z=55.6$  cm.

ured by replacing the boron coated hemispheres with uncoated iron ones. Background from possible polonium contamination on the boron target was measured by removing the Po source, and counting the neutrons still present. These measurements include, of course, the background of the counter when no source is present in the graphite column. The background from all causes was small as may be seen in Fig. 2.

## V. THE CROSS SECTION

In Fig. 3 is shown the cross section for the  $B^{10,11}(\alpha,n)N^{13,14}$  reactions as a function of the alpha-particle energy. The energy is the average energy of alpha-particles in the boron layer, taking into account energy losses in the Po source and in the boron layer, as well as in the nitrogen gas. Because of poor resolution, the cross section shown in Fig. 3 at a given energy is, of course, an average over a small energy interval determined by the resolution width. The cross section is:

$$\sigma = I/NS$$

where  $I$  is the number of neutrons emitted per second,  $S$  is the number of alpha-particles striking the boron per second, and  $N$  is the thickness of the target in boron atoms/cm<sup>2</sup>.

The alpha-particle energies corresponding to the four resonances suggested by curve 3 of Fig. 2, are listed in Table IV. For comparison are listed the eight resonances observed by Maurer<sup>2</sup> and those resonances observed by Fünfer<sup>3</sup> with  $ThC'$  alpha-particles, which lie below 5.3 Mev.

The fact that fewer resonances were observed in the present experiment than were found by Maurer and by

TABLE IV. Energy of the alpha-particles at resonance.

Present paper	Maurer*	Fünfer
1.8 Mev	1.90 Mev	
2.5	2.68	2.65 Mev
	3.15	3.25
	3.59	3.60
4.2	4.26	4.10
	4.55	4.45
	4.85	4.73
4.9	5.02	5.08

\* These energies, which differ slightly from those listed by Maurer, were found from Maurer's ranges using the newer range-energy relation given by Holloway and Livingston.<sup>4</sup>

Fünfer may be due to the relatively poor resolution indicated in Table III.

From the cross section,  $\sigma$ , as a function of the alpha-particle energy shown in Fig. 3, the total neutron yield from *Po* alpha-particles on a thick boron target has been calculated. The result is, for the thick target yield:

19 neutrons per  $10^6$ -*Po* alpha-particles.

This is in good agreement with the value of 22 neutrons per  $10^6$ -*Po* alpha-particles measured directly by Roberts<sup>6</sup> and 19 neutrons per  $10^6$ -*Po* alpha-particles found by Segrè and Wiegand.<sup>7</sup>

An estimate of the probable error in the cross-section shown in Fig. 3 is about 20 percent.

ACKNOWLEDGMENTS

I am indebted to Mr. Glen Barbaras and Dr. W. P. Jesse for making the boron layers; to Mr. Leonard Treiman and Professor Don Martin for making the polonium sources; and to Professor H. H. Barschall for suggesting the experiment, and interest in its progress.

APPENDIX

The use of thermal neutron measurements in a graphite column to obtain the approximate ratio of the strengths of two neutron sources, even though their energies may be different, is based upon an analysis which may be qualitatively outlined as follows:

As is well known, if a "point" source of fast neutrons is placed in a large graphite block, the neutrons will be slowed down by successive collisions with carbon nuclei until they reach thermal energies. Thereafter, they will diffuse in the graphite until they either are absorbed or escape from the block.

The distribution of thermal neutrons in the graphite column will depend upon the primary energy of the neutron source, because the higher the primary energy, the farther the neutrons will spread out from the source during the slowing down process. A measure of this spreading out may be obtained from the elementary age theory of the slowing down process.<sup>8,9</sup> According to

age theory, if a point source of neutrons of a single energy is placed in an infinitely large block of graphite, the spatial distribution of neutrons just reaching thermal energies, or the density of "nascent thermal neutrons,"  $q(\mathbf{r})$  is a Gaussian,

$$q(\mathbf{r}) = (Q/\pi^3 r_0^3) e^{-r^2/r_0^2}$$

where  $Q$  is the total number of neutrons emitted per second by the source. The parameter  $r_0$  is larger, the higher the primary energy of the neutrons. ( $r_0 = 2\tau^{\frac{1}{2}}$  where  $\tau$  is the neutron "age"). In a finite, but large, column such as used in the present experiment, the distribution  $q(\mathbf{r})$  is slightly different from the Gaussian given above, since it must satisfy boundary conditions that the neutron density vanish at the effective sides of the block. However, the age theory result<sup>8</sup> is characterized by the same parameter  $r_0 = 2\tau^{\frac{1}{2}}$  which appears in the simple Gaussian distribution for an infinite block.

$q(\mathbf{r})$  is important in calculating the distribution of thermal neutrons in the graphite column, since  $q(\mathbf{r})$  is the distributed source of thermal neutrons in the graphite. The distribution of thermal neutrons may be found by solving the steady state diffusion equation with source function  $q(\mathbf{r})$ :<sup>8</sup>

$$-D\nabla^2 n(\mathbf{r}) + (1/T)n(\mathbf{r}) = q(\mathbf{r})$$

where  $n(\mathbf{r})$  is the density of thermal neutrons at position  $\mathbf{r}$ ,  $D$  is the diffusion constant, and  $T$  is the mean life of the thermal neutrons in graphite. The boundary conditions are that  $n(\mathbf{r})$  vanish at the effective sides of the block.

By solving this equation using the age theory result for  $q(\mathbf{r})$ , one may calculate the flux,  $\nu v$ , of thermal neutrons at any point in the graphite, as a function of the parameter  $r_0$  in the source function,  $q(\mathbf{r})$ . The results of such a calculation are shown in Fig. 4 for four different distances from the source on the axis of the graphite column used in the present experiment.

By choosing a distance from the source for which the curve is as flat as possible over a large range in  $r_0$ , one may assume that the density of thermal neutrons at this position will be approximately proportional to the total source strength,  $Q$ , and will be insensitive to the primary energy of the neutrons.

For the distance between source and detector,  $z \approx 58$  cm, used in this experiment, the thermal flux curve is seen to be flat within about 10 percent for parameters  $r_0 \leq 45$  cm. Unfortunately it is not possible to say that this corresponds to a definite primary energy of the neutrons. According to the age theory approximation,  $r_0 = 42$  cm for neutrons of 4 Mev primary energy, in graphite, and increases only slowly with further increase in primary energy. However, if the actual distribution arising from a source of 4-Mev neutrons were expressed empirically by a sum of two or three Gaussian terms, one of them would probably have a parameter,  $r_0$ , considerably larger than 42 cm. It is felt, nevertheless, that the thermal neutron flux at  $z \approx 58$  cm varies with the primary neutron energy by less than ten to fifteen percent over the energy range of the neutrons produced in the present experiment.

Since a Ra- $\alpha$ -Be source (having a neutron spectrum extending to quite high energies) was used as a standard in the present experiments, it is of interest to compare with the curves of Fig. 4 the thermal neutron flux produced by a Ra- $\alpha$ -Be source. The distribution of nascent thermal neutrons,  $q(\mathbf{r})$ , from various Ra- $\alpha$ -Be sources have been measured experimentally so that the flux of thermal neutrons may be calculated with fair accuracy. The result for one particular Ra- $\alpha$ -Be source at a distance  $z = 55.6$  cm is indicated in Fig. 4. Since the flux from this source is seen to be 10 or 15 percent below that calculated for a source with small  $r_0$ , the value of the boron ( $\alpha, n$ ) cross section may be too high by about this amount, except near the high energy end.

<sup>6</sup> J. H. Roberts, Manhattan Project Report MDDC-731 (1944).

<sup>7</sup> E. Segrè and C. Wiegand, Manhattan Project Report MDDC-185 (1944).

<sup>8</sup> E. Fermi, Neutron Physics (Los Alamos Lecture Notes) MDDC-320 (1946).

<sup>9</sup> R. E. Marshak, Rev. Mod. Phys. 19, 185 (1947).